A Two-Particle Model for Rocket Plume Radiation

D. K. Edwards,* Y. Sakurai,† and D. S. Babikian‡
University of California, Irvine, California

A radiation model is proposed for the plumes of solid rocket motors firing into what is essentially a vacuum. The plume contains cold scattering particles and hot emitting/absorbing particles in overlapping conical clouds; the half-angle of the hot-particle cloud may be smaller than that of the cold-particle cloud. The clouds have axially varying radiative properties, with the hot particles imagined to lose emissive power and particle emissivity with increasing axial distance. Parametric calculations are made using the hybrid Monte Carlo, radiosity/irradiation technique to show which parameters are critical and how they may be inferred from engineering tests.

Nomenclature

B = blackbody emissive power σT^4, W/m^2
I = radiant intensity (radiance), W/m^2 · sr
J = radiosity, W/m^2
K = extinction coefficient, m^{-1}; with subscript, absorption or scattering coefficient, m^{-1}
M = number of Monte Carlo rays
n = power law exponent
N = number of surfaces and volumes
q = radiant flux, W/m^2
R = radial location, m
s = slant path, m
t = optical depth
T = temperature, K
z = distance from the apex of the cone along its surface, m
β = angle from conical axis
ϵ = emissivity
θ = polar angle from surface normal
π = 3.14159...
σ = Stefan-Boltzmann constant, W/m^2 · K^4
ϕ = azimuthal angle from cone generatrix ($\phi = 0$ is directed downstream)
ω = albedo for single scatter
Ω = solid angle, sr

Subscripts

a = absorption
b = Bobco
c = cold particles
e = exit reference condition
h = hot particles
i, j, k = ith, jth, or kth zone
mp = melting point
o = end of the line of sight
r = receiver
s = scattering
t = thermal black body emission

Superscripts

$()^+$ = outgoing
$()^-$ = incoming
$()'$, $()''$ = variable of integration

Introduction

THE Bobco engineering model for calculating plume radiation to aft-end equipment[1] has been employed in the aerospace industry for the past 18 years. In this model, as shown in Fig. 1, half-angle β, exit radius R_e, and the parameters exit plane radiosity J_e (in W/m^2) and radiosity decay exponent n_b must be specified. Thermal radiation to aft-end equipment is then calculated as if the plume were a perfectly diffuse solid wall. This simplicity facilitates fitting the model to the experimental data, and the ease of the numerical calculations required permits wide-ranging engineering studies to be made at low expense in computer time.

Concerns that the user of the model may have[2,3] are questions about the accuracy inherent in the assumption of perfectly diffuse radiant intensity I (plume radiosity per unit solid angle). It is granted that some angular variation in plume intensity can be accommodated in the decay exponent n_b. As lines of sight from an aft-end receiver move down the plume, angular intensity variation can appear as axial variation in diffuse radiosity. However, in an engineering model, one would prefer not to adjust J_e and n_b to accommodate different aft-end receiver locations; also azimuthal and polar angular variations of the plume intensity are a concern.

Despite these concerns, it is not easy to substitute an alternative to the Bobco model. Progress has been made toward developing exact calculations of plume radiation based upon detailed knowledge of particle optics, radiation transfer theory, and multiphase gas and particle dynamics; e.g., see Refs. 4-12. However, the phenomena occurring in solid rocket motor (SRM) plumes are complex. Molten liquid-oxide particles may have dissolved impurities in a suboxidized state. After primary combustion and agglomeration in the engine chamber and nozzle inlet, particles may be breaking up in the expansion cone and undergoing further chemical reactions. Phase change with zone refining within the particles occurs as they cool in the expanding plume gases. Thus, the particle sizes, compositions, temperatures, and structures are changing in the plume, as do their unknown optical properties.

In this paper, there is proposed a model based upon a conical cloud with critical axially varying properties. Sensitivity studies are presented to show that rather arbitrary assignment of all but two of the parameters can be made. Fast-running radiation line-of-sight calculations can be made with the model by fitting the scattering source functions for a number of conically annular zones with power law axial decay after

Presented as Paper 85-1069 at the AIAA 20th Thermophysics Conference, Williamsburg, VA, June 19-21, 1985; received Nov. 20, 1985; revision received Feb. 20, 1986.

*Professor of Mechanical Engineering, Associate Dean of Engineering. Associate Fellow AIAA.
†Visiting Scholar; Member, Technical Staff, Mitsubishi Electric Corp., Kamakura, Japan. Member AIAA.
‡Research Assistant, Department of Mechanical Engineering. Student Member AIAA.

having determined them via the hybrid Monte Carlo matrix inversion technique.[13] The conical cloud model is examined to discover departures from the simpler Bobco model and to explore the conditions under which these departures have engineering significance. Discussion is presented on how experimental measurements may be used to specify the parameters of the conical cloud model.

Physical Features to be Modeled

Heat radiation is emitted by hot particles as a continuum spectrum and by gases as vibration/rotation band spectra. The lines in the bands have a spectral width governed by collisional and Doppler broadening; these processes are enhanced by high pressure and high temperature. The bands have a spectral breadth governed by rotational excitation and their spectral locations are fixed by the vibrational energy level differences. In the plume of an SRM used for injection and thus firing into essentially a vacuum, the gases and small fine particles in them are cold relative to the original combustion chamber temperature. It is the large particles that, by virtue of their thermal mass, stay hottest for the longest times and distances in the plume. The large particles are both accelerated and cooled less rapidly than the small ones by the expanding gases in the thrust cone and beyond. Because the large particles move more slowly than the gases and fine particles, they are broken up and their numbers depleted. Upon breakup, the resulting fragments possess more radiative cross section. After perhaps a brief interval following breakup when some chemical heat liberation may occur, the fragments are certainly cooled by the surrounding cold gas, but the release of the latent heat of fusion holds the larger fragments at the melting point for some time and distance in the plume.

Not only do the hot particles have a much higher σT^4 than the cold fine particles; they have a much higher particle emissivity $\epsilon_h = (1 - \omega_h)$. Upon freezing completely, the finer particles are scattering, but only very weakly absorbing. Consequently, the emission from a vacuum-firing SRM is dominated by hot-particle radiation scattered by the surrounding cold particles.

An Engineering Model

An engineering model is necessarily a compromise between simplicity/utility and realism. The following model is proposed: hot particles have isotropic absorbing and scattering properties fixed by absorption coefficient K_{ha} and scattering coefficient K_{hs}. Cold particles have similar coefficients K_{ca} and K_{cs}. The total extinction coefficient is K, where

$$K = K_h + K_c = K_e(z_e/z)^2 \tag{1}$$

$$K_h = K_{ha} + K_{hs} = K_{he}(z_e/z)^2 \tag{2}$$

$$K_c = K_{ca} + K_{cs} = K_{ce}(z_e/z)^2 \tag{3}$$

where subscript e denotes the exit condition and z the distance from the apex of the cone measured along the surface of the cone. Extinction coefficient K is assumed to be uniform across the cone.

The cold particles are assumed to have albedo $\omega_c = 1$, where albedo $\omega = K_s/K$. The hot particles have an "emissivity" varying in a Bobco-like power law manner

$$\epsilon_h = 1 - \omega_h = \epsilon_{he}(z_e/z)^{n_h} \tag{4}$$

where $\epsilon_n = K_{ha}/K_h$. Here "particle emissivity" is used in the sense of Ref. 14. Moreover, the hot particles may be cooling in temperature as well. Provision is made by proposing

$$B_h = \sigma T_h^4 = B_e(z_e/z)^{n_t} \tag{5}$$

Finally, it is proposed that the hot particles may be confined to an inner core of half angle β_h. As described in the previous section, the hot particles are either large or the recent offspring of large hot parents and are still in the same neighborhood. The large particles tend to be confined to a central core because of their greater inertia against expansion in the nozzle cone.

Note that the surface radiosity of an infinite cylinder of radius R with a hot core of radius R_h under emitting thin conditions $K_{ha}R_h \ll 1$ is

$$J = 2R_h(1 - \omega_h)K_h B_h R_h/R \tag{6}$$

Applying this relation to a conical plume, one expects approximately

$$J = 2(R_h^2/R)\epsilon_{he}K_{he}B_e(z_e/z)^{n_h + n_t + 2}$$

or

$$J = 2(R_{he}^2/R_e)\epsilon_{he}K_{he}B_e(z_e/z)^{n_h + n_t + 1} \tag{7}$$

Accordingly, as definitions, one takes

$$n_b = n_h + n_t + 1 \tag{8}$$

$$\epsilon_e = 2(R_{he}^2/R_e)\epsilon_{he}K_{he} \tag{9}$$

$$J_e = \epsilon_e B_e \tag{10}$$

[Recall from Eq. (5) that B_e denotes σT_h^4 at the exit plane.] Here, n_b is the familiar Bobco decay exponent and J_e the exit emissivity of the plume. For convenience, the optical depth may be defined as

$$t_e = 2R_e K_e \tag{11}$$

In summary, the specification of the following parameters defines the plume model just described:

n_b = axial decay exponent, Eq. (8)

ϵ_e = plume emissivity, Eq. (9)

J_e = plume radiosity, Eq. (10)

t_e = plume optical depth, Eq. (11)

ϵ_{ha} = hot particle emissivity, Eq. (4)

n_t = source decay exponent, Eq. (5)

β = cone half angle

β_h = hot zone half angle

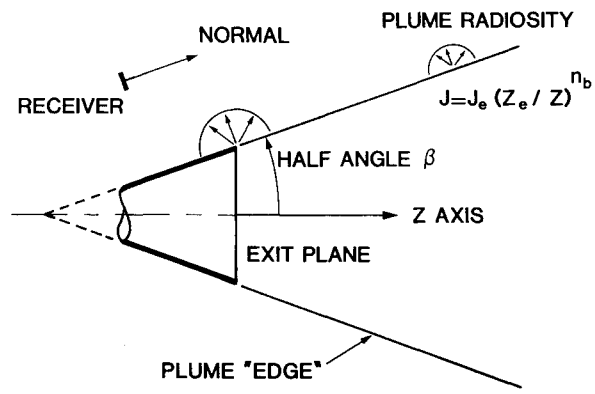

Fig. 1 Bobco plume model.

These specifications are sufficient to define the values of K_{cs} ($K_{ca}=0$), K_{ha}, K_{hs}, and B and how they vary with distance z. In what follows, it will be shown that n_b, J_e, and β are of prime importance, as one would expect from the success of the Bobco model, and that the rather arbitrary assignment of the remaining parameters has little consequence when t_e is sufficiently large. However, the results show conditions under which departures from the Bobco model may be expected and the forms that these departures take.

Use of the Model

The model may be executed using the hybrid Monte Carlo radiosity-irradiation formulation[13] summarized in the Appendix. In this formulation, the plume is divided into a number of zones as shown in Fig. 2. Making use of only the plume half-angle β, the zonal geometry, the optical depth t_e, and Eq. (1), one finds volume-to-volume shape factors. It is emphasized that in the calculations only straight-line paths are traced; no random-walk ray tracings are made. Consequently, the computation proceeds rapidly on even a small computer. Once the "shape factors" are computed and stored, wide-ranging parametric calculations can be made extremely rapidly. Making use of the shape factors, one finds the "particle radiosity" defined by the source terms in the equation of transfer

$$\frac{\mathrm{d}I}{\mathrm{d}s} = -KI + \frac{K_{ha}B_h}{\pi} + (\omega_h K_h + \omega_c K_c)\frac{1}{4\pi}\int_0^{4\pi} I\,\mathrm{d}\Omega \quad (12)$$

These terms (multiplied by π) are the particle radiosity q^+,

$$q^+ = K_{ha}B_h + (\omega_h K_h + \omega_c K_c)\frac{1}{4\pi}\int_0^{4\pi} I\,\mathrm{d}\Omega \quad (13)$$

where $\mathrm{d}\Omega$ denotes differential solid angle, $\sin\theta\,\mathrm{d}\theta\,\mathrm{d}\phi$ in the polar coordinates; see for example, Refs. 15 and 16.

Once q^+ is known as a function of z in the plume, Eq. (12) may be integrated readily. For the intensity of the irradiation emerging from the plume, one has from Eq. (12)

$$\pi I^- = \pi I_o e^{-t} + \int_0^t e^{-t'} q^+(t')\,\mathrm{d}t' \quad (14)$$

where t' is the optical depth along a line of sight of slant path s',

$$t' = \int_0^{s'} K\,\mathrm{d}s'' \quad (15)$$

and t is the total optical depth passing through the plume to either space or a hard body such as the thrust cone. In the calculations that follow, the hard-body intensity I_o was considered negligible. In integrating Eqs. (14) and (15), the variation with z indicated by Eq. (1) is taken into account. In the final integration of Eq. (14), the zonal values of particle radiosity are interpolated logarithmically in the z direction and linearly in the R direction.

To determine the irradiation q^- upon aft-end equipment, one integrates the intensity in the usual way,[1,2]

$$q^- = \int_0^{2\pi} I^- \cos\theta_r\,\mathrm{d}\Omega \quad (16)$$

where θ_r is the angle of incidence from the receiver surface normal.

Results and Discussion

The results are arranged so to examine the effects of the variation of each parameter. Table 1 shows the results of varying n_b, the Bobco axial decay exponent. Of particular interest in Table 1a is the particle radiosity of zone 20 at the exit of the thrust cone as shown in Fig. 2. As n_b increases from 1 to 3 the particle radiosity increases only 8%, presumably due to "searchlight effect," that is, the diffusion of radiation from the hotter, denser, and more emissive portions

Table 1 Effect of axial decay
($t_e=4$, $\epsilon_e=0.1$, $n_t=0$, $\epsilon_{he}=1$, $\beta=\beta_h=20$ deg)

a) Upon zonal particle radiosities

Zone no., k	Particle radiosity, q_k^+/B_e		
	$n_b=1$	$n_b=2$	$n_b=3$
13	0.202	0.274	0.367
14	0.172	0.233	0.316
15	0.140	0.193	0.264
16	0.100	0.139	0.193
17	0.132	0.136	0.147
18	0.116	0.118	0.127
19	0.099	0.101	0.108
20	0.077	0.078	0.083
21	0.089	0.064	0.050
22	0.082	0.058	0.045
23	0.072	0.051	0.039
24	0.059	0.042	0.031

b) Upon aft-end irradiation

Radial location, R/R_e	Axial location, z/z_e	Irradiation upon receiver $(q_r^-/B_e)\times 100$		
		$n_b=1$	$n_b=2$	$n_b=3$
2	0	0.467	0.294	0.215
	0.5	0.956	0.646	0.501
	1.0	1.997	1.363	1.056
3	0	0.546	0.334	0.240
	0.5	0.907	0.572	0.421
	1.0	0.121	0.707	0.480
4	0	0.517	0.305	0.213
	0.5	0.716	0.420	0.292
	1.0	0.814	0.430	0.267

Table 2 Effect of particle temperature decay instead of particle emissivity decay
($t_e=4$, $\epsilon_e=0.1$, $n_b=2$, $\epsilon_{he}=1$, $\beta=\beta_h=20$ deg)

a) Upon zonal particle radiosities

Zone no., k	Particle radiosity, q_k^+/B_e		
	$n_t=0$	$n_t=0.5$	$n_t=1$
13	0.274	0.300	0.330
14	0.233	0.252	0.276
15	0.193	0.206	0.224
16	0.139	0.148	0.158
17	0.136	0.139	0.143
18	0.118	0.121	0.124
19	0.101	0.103	0.106
20	0.078	0.080	0.081
21	0.064	0.064	0.064
22	0.058	0.058	0.058
23	0.051	0.051	0.051
24	0.042	0.042	0.042

b) Upon aft-end irradiation

Radial location, R/R_e	Axial location, z/z_e	Irradiation upon receiver $(q_r^-/B_e)\times 100$		
		$n_t=0$	$n_t=0.5$	$n_t=1$
2	0	0.294	0.294	0.295
	0.5	0.646	0.649	0.652
	1.0	1.363	1.368	1.374
3	0	0.334	0.335	0.336
	0.5	0.572	0.574	0.575
	1.0	0.707	0.707	0.707
4	0	0.305	0.305	0.305
	0.5	0.420	0.421	0.421
	1.0	0.430	0.430	0.429

Table 3 Effect of exit emissivity
($t_e = 4$, $n_b = 2$, $n_t = 0$, $\epsilon_{he} = 1$, $\beta = \beta_h = 20$ deg)

a) Upon zonal particle radiosities

Zone no., k	Particle radiosity, q_k^+ / B_e		
	$\epsilon_e = 0.1$	$\epsilon_e = 0.2$	$\epsilon_e = 0.3$
13	0.274	0.437	0.522
14	0.233	0.381	0.489
15	0.193	0.321	0.418
16	0.139	0.238	0.318
17	0.136	0.239	0.325
18	0.118	0.211	0.289
19	0.101	0.182	0.252
20	0.078	0.143	0.200
21	0.064	0.121	0.172
22	0.058	0.110	0.158
23	0.051	0.097	0.139
24	0.042	0.079	0.115

b) Upon aft-end irradiation

Radial location, R/R_e	Axial location, z/z_e	Irradiation upon receiver $(q_r^- / B_e) \times 100$		
		$\epsilon_e = 0.1$	$\epsilon_e = 0.2$	$\epsilon_e = 0.3$
2	0	0.294	0.559	0.804
	0.5	0.646	1.222	1.749
	1.0	1.363	2.573	3.679
3	0	0.334	0.636	0.916
	0.5	0.572	1.085	1.559
	1.0	0.707	1.351	1.952
4	0	0.305	0.581	0.837
	0.5	0.420	0.801	1.154
	1.0	0.430	0.828	1.203

Table 4 Effect of optical depth
($\epsilon_e = 0.1$, $n_b = 2$, $n_t = 0$, $\epsilon_{eh} = 1$, $\beta = \beta_h = 20$ deg)

a) Upon zonal particle radiosities

Zone no., k	Particle radiosity, q_k^+ / B_e		
	$t_e = 4$	$t_e = 2$	$t_e = 1$
13	0.274	0.257	0.291
14	0.233	0.230	0.273
15	0.193	0.204	0.257
16	0.139	0.167	0.230
17	0.136	0.136	0.170
18	0.118	0.125	0.163
19	0.101	0.114	0.156
20	0.078	0.099	0.144
21	0.064	0.072	0.100
22	0.058	0.068	0.098
23	0.051	0.063	0.094
24	0.042	0.056	0.089

b) Upon aft-end irradiation

Radial location, R/R_e	Axial location, z/z_e	Irradiation upon receiver $(q_r^- / B_e) \times 100$		
		$t_e = 4$	$t_e = 2$	$t_e = 1$
2	0	0.294	0.287	0.284
	0.5	0.646	0.626	0.617
	1.0	1.363	1.299	1.254
3	0	0.334	0.322	0.316
	0.5	0.572	0.545	0.529
	1.0	0.707	0.668	0.642
4	0	0.305	0.290	0.282
	0.5	0.420	0.397	0.382
	1.0	0.430	0.405	0.387

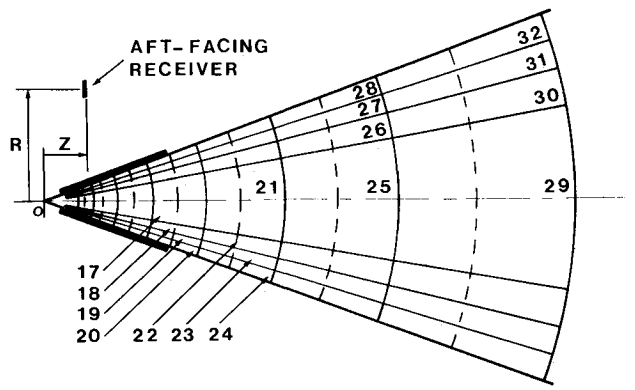

Fig. 2 Plume model geometry (solid lines show zone boundaries and dashed lines pass through zone centroids; zones are numbered).

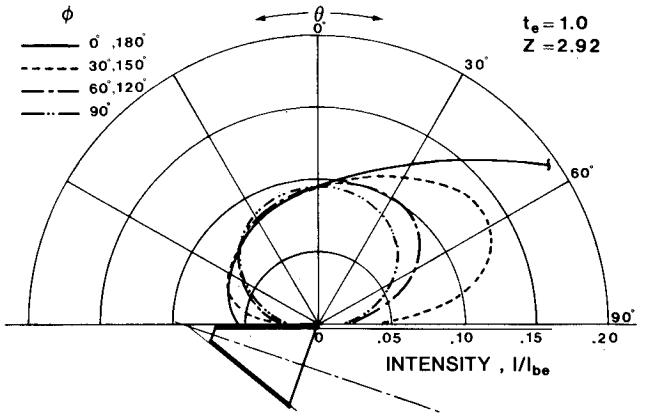

Fig. 3 Directional variation of plume intensity, $t_e = 1.0$ (azimuthal angles $\theta = 0$-90 deg are on the right of the polar plot for the intensity directed downstream, azimuthal angles $\theta = 90$-180 deg on the left for the intensity directed upstream; the polar plot shows $I/I_{be} = \pi I/B_e$, $n_b = 2$, $\epsilon_e = 0.1$, $n_t = 0$, $\beta = \beta_h = 20$ deg).

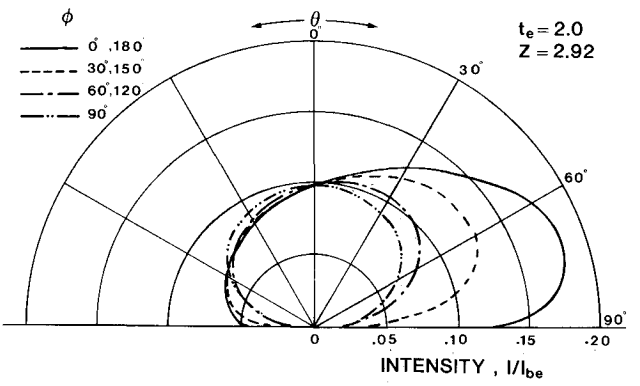

Fig. 4 Directional variation of plume intensity, $t_e = 2.0$ (see explanatory note on Fig. 3).

of the plume to the cooler portions. The irradiation upon an aft-facing receiver is, of course, strongly influenced. Table 1b shows the value to fall from 0.00467 to 0.00215 for a far-forward location. (Note that the table values are times 100.)

Table 2 shows the effect of varying n_t at constant n_b. Again, attention is directed to zone 20. Only a 4% change is seen. Since n_b is constant, there is little change seen in Table 2b. This null result is very significant. It suggests that there should be no concern about getting correct values for both ϵ_e and B_e and for both n_t and n_h. Doing so poses an extremely difficult task. But it is necessary only to get their product and n_b correct from easy experimental measurements. Two radiometers, one looking in the vicinity of z_e and the other at, say, $2z_e$, will serve to fix both J_e and n_b.

Superficially, Table 3 might suggest that ϵ_e is a large factor —and so it is at constant B_e. But, if one examines Table 3b dividing the first column by 0.1, the second by 0.2, and the third by 0.3 (that is, to express the results as q_r^- / J_e), one sees only a small effect. Table 3a, zone 20, shows a $\sqrt{1 - \omega_h}$ variation as expected; see, e.g., Refs. 7 and 17.

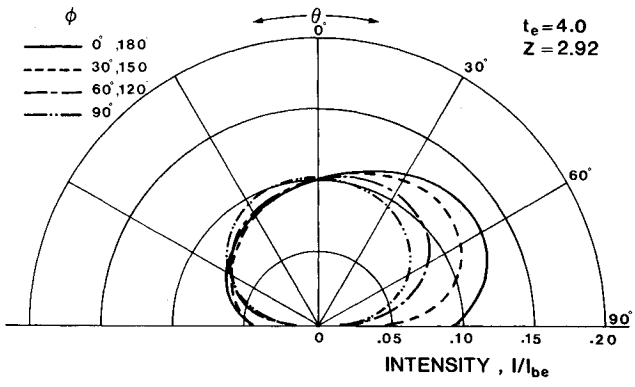

Fig. 5 Directional variation of plume intensity, $t_e = 4.0$ (see explanatory note on Fig. 3).

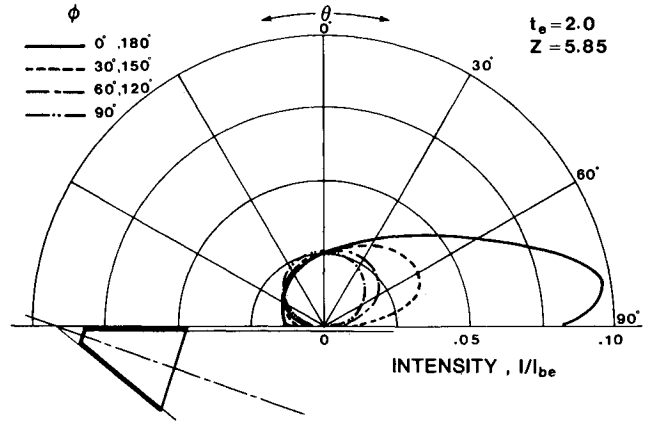

Fig. 6 Directional variation of plume intensity at a downstream location, $t_e = 2.0$ (see explanatory note on Fig. 3).

The data in Table 4a show the expected increase when the optical depth drops to unity at constant ϵ_e, while that in Table 4b do not show much effect. However, a dramatic effect is seen in Figs. 3-5. The intensity viewed when looking into the thrust cone departs greatly from the diffuse Bobco model. It is remarkable, however, how little the forward-directed intensity varies as the optical depth is decreased and how little azimuthal variation there is. Only at polar angles of 70 deg or more and at the low optical depths does the variation with the azimuthal angle ϕ become large. The reason for this insensitivity to ϕ is that less axial decay in the source function is seen as ϕ is rotated to 90 deg, thus, in part, offsetting the loss of optical depth for the shorter paths through the plume.

There is evident in the forward direction a significant variation with polar angle. In Fig. 3, for $t_e = 4$ at $\theta = 0$, the intensity is $\pi I^-/B_e = 0.10$ in keeping with the $\epsilon_e = 0.1$ emissivity value. At an angle of $\theta = 60$ deg, the value is 0.07, and it falls to 0.06 at 75 deg. It had been recommended[2] to assume that the intensity falls as $(1 + \cos\theta)/2$, based upon the Chandrasekhar H functions,[17] but the variation observed in Fig. 3 exceeds that, presumably due to the axial decay in the source function. The effect of low t_e is more evident at higher values of z, as indicated in Fig. 6.

Table 5a shows little variation of particle radiosity with varying plume half-angle at constant t_e and ϵ_e. This lack of variation is expected, because the plume optics should be largely determined by the optical depth and albedo, despite the axial variations. This insensitivity does not carry over to the irradiation values because the solid angle subtended by the plume is increased in Eq. (16). Thus, at receiver locations far forward, the flux received is sensitive to plume angle.

The effect of ϵ_{he} is negligibly small as long as ϵ_e is low and t_e large. The scattering contributed by the hot particles cannot

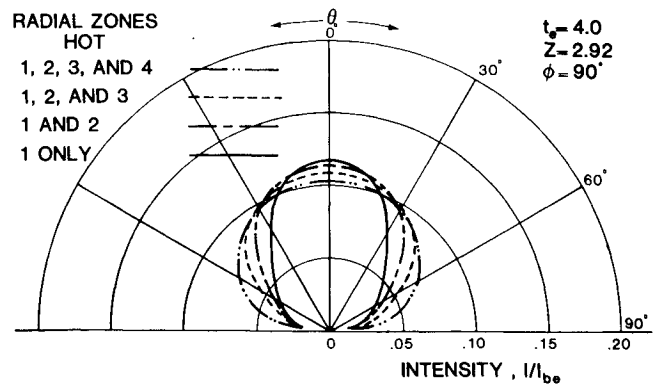

Fig. 7 Effect of radial source variation on plume intensity ($t_e = 4.0$, $n_b = 2$, $\epsilon_e = 0.1$, $n_t = 0$).

Table 5 Effect of cone angle ($t_e = 4$, $\epsilon_e = 0.1$, $n_b = 2$, $n_t = 0$, $\epsilon_{eh} = 1$, $\beta_h = \beta$)

a) Upon zonal particle radiosities

Zone no., k	Particle radiosity, q_k^+/B_e		
	$\beta = 15$ deg	$\beta = 20$ deg	$\beta = 25$ deg
13	0.274	0.274	0.273
14	0.234	0.233	0.233
15	0.192	0.193	0.193
16	0.139	0.139	0.139
17	0.135	0.136	0.136
18	0.118	0.118	0.119
19	0.101	0.101	0.102
20	0.078	0.078	0.078
21	0.064	0.064	0.065
22	0.058	0.058	0.059
23	0.051	0.051	0.051
24	0.041	0.042	0.042

b) Upon aft-end irradiation

Radial location, R/R_e	Axial location, z/z_e	Irradiation upon receiver $(q_r^-/B_e) \times 100$		
		$\beta = 15$ deg	$\beta = 20$ deg	$\beta = 25$ deg
2	0	0.186	0.294	0.408
	0.5	0.456	0.646	0.806
	1.0	1.392	1.363	1.341
3	0	0.237	0.334	0.412
	0.5	0.491	0.572	0.608
	1.0	0.758	0.707	0.666
4	0	0.245	0.305	0.336
	0.5	0.410	0.420	0.409
	1.0	0.481	0.430	0.390

be distinguished from that of the cold particles in a model that postulates uniform dispersion over β. However, even when the hot particles are confined to the inner zones, there is little effect to be seen at fixed low ϵ_e and large t_e. When one considers spectral (wavelength) variation, one should note that as wavelength is increased, scattering and thus total optical depth t_e fall rapidly. Thus the insensitivity of aft-end equipment heating to details of the plume flow would not carry over to infrared diagnostics.

Figure 7 shows the effect of β_h being less than β. The parameters correspond to those of the $\phi = 90$ deg curve of Fig. 5. Shown in Fig. 7 are four curves corresponding to $\beta_h = 20$, 17.3, 14.1, and 10 deg. These values were chosen to correspond to 1.0, 0.75, 0.50, and 0.25 of the volume of the plume. As the volume containing hot particles is reduced to 0.25, the radiant intensity at angles larger than 45 deg from the conical plume surface normal falls by 35% and the normal intensity rises by 12%. For the same parameters, at a z station twice as large, the elongation of the lobe in the normal direction becomes considerably greater, rising by 41% rather than 12%. It is suggested that $\phi = 90$ deg ground test data

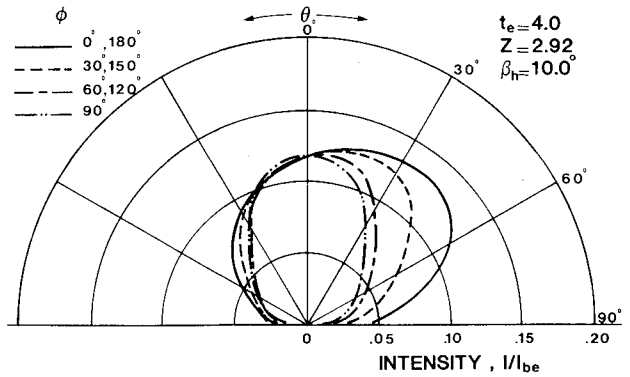

Fig. 8 Directional variation of plume intensity with hot inner core ($t_e = 4.0$, $n_b = 2$, $\epsilon_e = 0.1$, $n_t = 0$).

variations with θ can be used as a guide for deciding upon a value of β_h.

Figure 8 shows the polar and azimuthal diagram corresponding to the conditions of Fig. 5, but with $\beta_h = 10$ deg. For an azimuth $\phi = 0$ deg in a plane containing the plume axis, beyond $\theta = 35$ deg, the radiant intensity for $\beta_h = 10$ deg falls below that for $\beta_h = 20$ deg. For example, at $\theta = 60$ deg, the ratio is about 0.75. At more normal angles, the reverse is true. At $\theta = 0$ deg, the value for $\beta_h = 10$ deg is 12% above that for $\beta_h = 20$ deg, as already noted. These variations can be compared to flight test data to confirm a value of β_h.

In view of the parametric studies presented here, one would believe that critical engineering data for a given SRM would include 1) a measurement of plume intensity at two axial locations to fix J_e and n_b, 2) a measurement of plume intensity looking up into the thrust cone to determine whether or not t_e is large, 3) measured values of radiant intensity versus polar angle at a fixed axial station for a convenient azimuth to help fix β_h, and 4) a measurement of hemispherical irradiation at a far forward receiver location to help fix β. These measurements leave unresolved the values of ϵ_e and B_e separately, but they are seen here to be of little consequence. For high expansion ratio "cold" motors (with low values of J_e), the value of B_e is probably that for the melting point T_{mp} of the metal oxides, $B_e = \sigma T_{mp}^4$ and ϵ_e is of order 0.1. For low expansion "hot" motors (with large values of J_e), both values are considerably higher; perhaps, the geometric mean of the chamber temperature and melting point can be used to fix arbitrarily B_e and ϵ_e can be adjusted to agree with the measured value of J_e. Again, how much of n_b is to be associated with n_t and how much with n_h is a question difficult to resolve experimentally, but one with little consequence upon aft-end heating. Accordingly, it is suggested that for high-expansion cold motors $n_t = 0$ be used in keeping with the idea that B_h is constant at σT_{mp}^4, while for low-expansion hot motors n_t and n_h can be taken as equal and found from n_b via Eq. (8).

Conclusion

The results of this parametric study suggest that the Bobco engineering model for calculating plume radiation to aft-end equipment can continue to be used with some confidence with the proviso that, under scattering-thick/emitting-thin conditions, the plume surface emissivity should be taken to vary with angle θ. Figures 3-5 illustrate the θ variation for $t_e = 1$, 2, and 4 and $n_b = 2$.

For smaller motors with more optically thin plumes, the model proposed here can be employed more reasonably. The model here makes provision for cooling particles losing emissive power through loss of both particle emissivity and blackbody radiosity and automatically makes provision for the θ, ϕ variation of the plume intensity. It has been shown how the critical parameters of the model can be fixed from engineering experiments and how other less critical parameters can be set reasonably. By use of the particle radiosity-irradiation formulation of Ref. 13, calculations based upon the model can be carried out even on a small computer.

Appendix

The hybrid Monte Carlo matrix-inversion formulation of radiation heat transfer with volume scattering[13] is summarized. First, the standard engineering radiosity-irradiation formulation[18-21] is briefly stated and the standard Monte Carlo method summarized[22-28]; then, starting with the equation of transfer, it is shown how volume scattering is included.

Radiosity q_i^+ for a perfectly diffuse surface is π times the outgoing intensity I_i^+ and is composed of emitted and reflected radiation. The emissivity for an opaque surface can be written as absorptivity $(1 - \rho_i)$ with Kirchhoff's law. Accordingly, the radiosity equation is

$$q_i^+ = (1 - \rho_i) B_i + \rho_i q_i^- \tag{A1}$$

The irradiation q_i^- is composed of contributions from the other sources,

$$q_i^- = \sum_j F_{i-j} q_j^+ \tag{A2}$$

where the shape factor F_{i-j} is an integral over the solid angle subtended by the jth source, averaged over the surface of surface i,

$$F_{i-j} = \frac{1}{A_i} \int_{A_i} \frac{1}{\pi} \int_{\Omega_j} \cos\theta \, d\Omega \, dA_i \tag{A3}$$

Here $\cos\theta$ is the projection of a ray from i to j onto the normal to surface i. It is seen that Eqs. (A1) and (A2) are $2N$ equations ($i = 1$ to N) in $2N$ unknowns. Matrix inversion provides a solution, provided the values of ρ_i, B_i, and F_{i-j} are known.

Shape factor F_{i-j} is found with the Monte Carlo method by sending forth M "rays" or "photon bundles" from surface i and finding how many directly strike surface j,

$$F_{i-j} = M_j / M \tag{A4}$$

In view of Eq. (A4), the origins of the rays are randomly selected on surface i in such a way that the density of points is uniform as M goes to infinity. The $\cos\theta \, d\Omega$ product in polar coordinates is

$$\cos\theta \, d\Omega = \cos\theta \sin\theta \, d\theta \, d\phi \tag{A5}$$

Accordingly, the appropriate fractional functions to select angles ϕ and θ are

$$f_\phi = \frac{\int_0^\phi d\phi}{\int_0^{2\pi} d\phi}, \qquad f_\theta = \frac{\int_0^\theta \cos\theta \sin\theta \, d\theta}{\int_0^{\pi/2} \cos\theta \sin\theta \, d\theta}$$

$$\phi = 2\pi f_\phi, \qquad \sin^2\theta = f_\theta \tag{A6}$$

Uniform random selection of f_ϕ and f_θ thus fix values of θ and ϕ, fixing each ray to trace. Each time a ray encounters surface j, the value of M_j rises in the computer calculation.

The equation of transfer in a volume having extinction coefficient K and albedo for single scatter ω gives the change in radiant intensity I along slant path s.

For isotropic scattering

$$\frac{dI}{ds} = -KI + (1 - \omega) KI_t - \frac{\omega K}{4\pi} \int_0^{4\pi} I \, d\Omega \tag{A7}$$

A first step to formulate the scattering problem in terms of radiosity and irradiation is to define "irradiation" within a small volume numbered i as

$$q_i^- = \pi \bar{I} = \frac{\pi}{4\pi} \int_0^{4\pi} I \, d\Omega \tag{A8}$$

Then, with $B_i = \pi I_i$ in the ith volume, the "radiosity" is defined as

$$q_i^+ = \pi I_i^+ = (1 - \omega_i) \pi I_i + \frac{\pi \omega_i}{4\pi} \int_0^{4\pi} I \, d\Omega$$

$$q_i^+ = \pi I_i^+ = (1 - \omega_i) B_i + \omega_i q_i^- \tag{A9}$$

These definitions allow Eq. (A7) to be written as

$$\frac{dI}{ds} = -KI + KI_i^+ = -KI + \frac{Kq_i^+}{\pi} \tag{A10}$$

Equation (A10) is now solved for the radiant intensity received at a point where s is taken to be zero,

$$I^- = \int_0^s e^{-\int_0^{s'} K \, ds''} I^+(s') K \, ds' \tag{A11}$$

Extract from Eq. (A11) the contribution of the increment of path passing through the jth zone. Optical depth t is defined according to Eq. (15); the path from the origin in zone i to the entrance zone j is denoted $t_{i-j,1}$; and that to the exit is $t_{i-j,2}$. Thus, the contribution is

$$I_{i,j}^- = I_j^+ \left(e^{-t_{i-j,1}} - e^{-t_{i-j,2}} \right) \tag{A12}$$

In view of Eqs. (A11) and (A12), Eq. (A8) is written

$$q_i^- = \sum_j F_{i-j} q_j^+ \tag{A13}$$

Monte Carlo calculation of the volume shape factors F_{i-j} is made by choosing a point of origin randomly in volume i. Because Eq. (A8) has no $\cos\theta$ weighting, the appropriate value of f_θ becomes

$$f_\theta = \frac{\int_0^\theta \sin\theta \, d\theta}{\int_0^\pi \sin\theta \, d\theta} = \frac{(1 - \cos\theta)}{2}$$

$$\cos\theta = 1 - 2f_\theta \tag{A14}$$

This relation replaces the corresponding one in Eq. (A6). The ray is traced, with optical depth along it computed according to Eq. (15). Contributions to M_j are scored according to Eq. (A12) as

$$\Delta M_j = e^{-t_{i-j,1}} - e^{-t_{i-j,2}} \tag{A15}$$

When an opaque surface is encountered, $t_{i-j,2}$ is infinite and the second term is Eq. (A15) is zero.

The hybrid Monte Carlo matrix inversion formulation is thus clear. Shape factors are Monte Carlo calculated by choosing a point and direction as appropriate for a surface or volume source, Eq. (A6) or Eq. (A14). Ray tracing proceeds according to Eq. (A15), and Eq. (A4) gives F_{i-j}. The radiosity equations (A1) or (A9) require the reflectivities to be ρ_j for a surface and ω_j for a volume. Note that for the mixture of particles the effective values are

$$\omega = (\omega_h K_h + \omega_c K_c)/K \tag{A16}$$

$$B = \frac{(1 - \omega_h) K_h B_h + (1 - \omega_c) K_c B_c}{(1 - \omega) K} \tag{A17}$$

The radiosity equations and the irradiation equations (A2) or (A13) are solved by a standard matrix inversion to yield the radiosities, and these enter Eq. (14), allowing a standard line-of-sight integration to be executed without complication from the scattering.

Acknowledgments

The authors gratefully acknowledge Mrs. Verna Bruce for the preparation of the manuscript.

References

[1] Bobco, R.P., "Radiation from Conical Surfaces with Nonuniform Radiosity," *AIAA Journal*, Vol. 4, March 1966, pp. 544-546.

[2] Edwards, D.K., "Comment on 'Radiation from Conical Surfaces with Nonuniform Radiosity'," *AIAA Journal*, Vol. 7, Aug. 1969, pp. 1656-1659.

[3] Bobco, R.P., "Reply by author to D.K. Edwards," *AIAA Journal*, Vol. 7, Aug. 1969, p. 1659.

[4] Gryvnak, D.A. and Burch, D.E., "Optical and Infrared Properties of Al_2O_3 at Elevated Temperatures," *Journal of the Optical Society of America*, Vol. 55, June 1965, pp. 625-629.

[5] Plass, G.N., "Temperature Dependence of the Mie Scattering and Absorption Cross Sections for Aluminum Oxide," *Applied Optics*, Vol. 4, Dec. 1965, pp. 1616-1619.

[6] Carlson, D.J., "Radiation from Rocket Exhaust Plumes, Part II: Metallized Solid Propellants," AIAA Paper 66-652, 1966.

[7] Edwards, R.H. and Bobco, R.P., "Radiant Heat Transfer from Isothermal Dispersions with Isotropic Scattering," *Journal of Heat Transfer*, Vol. 89, Nov. 1967, pp. 300-308.

[8] Stockham, L.W. and Love, T.J., "Radiative Heat Transfer from a Cylindrical Cloud of Particles," *AIAA Journal*, Vol. 6, Oct. 1968, pp. 1935-1940.

[9] Pearce, B.E., "Radiative Heat Transfer within a Solid-Propellant Rocket Motor," *Journal of Spacecraft and Rockets*, Vol. 15, Jan.-Feb. 1978, pp. 125-128.

[10] Ludwig, C.B., Malkmus, W., Walker, J., Slack, M., and Reed, R., "A Theoretical Model for Absorbing, Emitting, and Scattering Plume Radiation," *AIAA Progress in Astronautics and Aeronautics: Spacecraft Radiative Transfer and Temperature Control*, Vol. 83, edited by T.E. Horton, AIAA, New York, 1982, pp. 111-127.

[11] Edwards, D.K. and Bobco, R.P., "Effect of Particle Size Distribution on the Radiosity of Solid Propellant Rocket Motor Plumes," *AIAA Progress in Astronautics and Aeronautics: Spacecraft Radiative Transfer and Temperature Control*, edited by T.E. Horton, Vol. 83, AIAA, New York, 1982, pp. 169-188.

[12] Nelson, H.F., "Influence of Particulates on Infrared Emission from Tactical Rocket Exhausts," *Journal of Spacecraft and Rockets*, Vol. 21, Sept.-Oct. 1984, pp. 425-432.

[13] Edwards, D.K., "Hybrid Monte-Carlo Matrix-Inversion Formulation of Radiation Heat Transfer with Volume Scattering," *Proceedings of ASME 23rd National Heat Conference*, HTD-Vol. 45, ASME, New York, 1985, pp. 273-278.

[14] Morizumi, S.J. and Carpenter, H.J., "Thermal Radiation from the Exhaust Plume of an Aluminized Composite Propellant Rocket," *Journal of Spacecraft and Rockets*, Vol. 1, Sept.-Oct. 1964, pp. 501-507.

[15] Edwards, D.K., *Radiation Heat Transfer Notes*, Hemisphere Publishing Corp., New York, 1981.

[16] Siegel, R. and Howell, J.R., *Thermal Radiation Heat Transfer*, 2nd ed., Hemisphere/McGraw-Hill, New York, 1981.

[17] Chandrasekhar, S., *Radiative Transfer*, Dover Publications, New York, 1960.

[18] Hottel, H.C., and Sarofim, A.F., *Radiative Transfer*, McGraw-Hill Book Co., New York, 1967.

[19] Oppenheim, A.K., "The Engineering Radiation Problem—An Example of the Interaction Between Engineering and Mathematics," *Zeitschrift für Angewandte Mathematik und Mechanik*, Vol. 36, March-April 1956, pp. 81-83.

[20] Ishimoto, T. and Bevans, J.T., "Method of Evaluating Script-F for Radiant Exchange within an Enclosure," *AIAA Journal*, Vol. 1, June 1963, pp. 1428-1429.

[21]Bobco, R.P., "Radiation Heat Transfer in Semigray Enclosures with Specularly and Diffusely Reflecting Surfaces," *Journal of Heat Transfer*, Vol. 86, Feb. 1964, pp. 123-130.

[22]Howell, J.R. and Perlmutter, M., "Monte Carlo Solution of Thermal Transfer Through Radiant Media Between Gray Walls," *Journal of Heat Transfer*, Vol. 86, Feb. 1964, pp. 116-122.

[23]Howell, J.R., "Application of Monte Carlo to Heat Transfer Problems," *Advances in Heat Transfer*, Vol. 5, 1966, pp. 1-54.

[24]Corlett, R.C., "Direct Monte Carlo Calculation of Radiative Heat Transfer in Vacuum," *Journal of Heat Transfer*, Vol. 88, Nov. 1966, pp. 376-382.

[25]Toor, J.S. and Viskanta, R., "A Numerical Experiment of Radiant Heat Exchange by the Monte Carlo Method," *International Journal of Heat and Mass Transfer*, Vol. 11, May 1968, pp. 883-897.

[26]Look, D.C. and Love, T.J., "Investigation of the Effects of Surface Roughness upon Reflectance," *AIAA Progress in Astronautics and Aeronautics: Heat Transfer and Spacecraft Thermal Control*, Vol. 24, edited by J.W. Lucas, AIAA, New York, 1971, pp. 123-142.

[27]Edwards, D.K. and Bertak, I.V., "Imperfect Reflections in Thermal Radiation Transfer," *AIAA Progress in Astronautics and Aeronautics: Heat Transfer and Spacecraft Thermal Control*, Vol. 24, edited by J.W. Lucas, AIAA, New York, 1971, pp. 143-163.

[28]Richter, W. and Heap, M., "A Semistochastic Method for the Prediction of Radiative Heat Transfer in Combustion Chambers," Paper 81-17 presented at Spring Meeting, Western States Section, Pullman, WA, The Combustion Institute, 1981.